

Effects of Charge Exchange in $^{90,91}\text{Zr}(d,p)^*$

R. G. Clarkson†, W. R. Coker, and C. F. Moore

Center for Nuclear Studies, The University of Texas, Austin, Texas 78712

(Received 30 July 1969; revised manuscript received 11 June 1970)

An extensive study of $^{90,91}\text{Zr}(d,p)$ excitation functions has been carried out for deuteron energies from 5 to 11 MeV, in order to investigate the extent and systematic behavior of charge-exchange contributions to the (d,p) process. Nine residual states in ^{91}Zr , up to excitations of 3.7 MeV, were involved, as well as three residual states of ^{92}Zr , up to 1.5 MeV in excitation. In addition, deuteron elastic scattering from ^{90}Zr and ^{91}Zr was measured from 5 to 11.0 MeV, and proton elastic scattering from 9.5 to 14.0 MeV. Energy-dependent optical potentials were extracted from the elastic scattering data, and distorted-wave Born approximation analyses were performed for the (d,p) data. An effort is made to demonstrate and summarize the various factors contributing to the manifestation of the charge-exchange threshold effect in (d,p) . To provide the necessary perspective, a considerable amount of other data bearing on the nature of the effect is briefly described, including possible observation of charge-exchange effects with mass-50 targets, comparison of $(p,n\bar{p})$ and $(\bar{d},n\bar{p})$ excitation curves near threshold, and resonance behavior in (p,p) and (d,p) , which can confuse the experimental and theoretical situation. The experimental evidence is concluded to be consistent with the Lane model of such processes, suggested by Zaidi and von Brentano.

I. INTRODUCTION

The initial suggestion that charge exchange could couple analogous (d,p) and (d,n) channels was given by Moore *et al.*,¹ who reported the experimental observation of a marked dip in the $^{90}\text{Zr}(d,p)^{91}\text{Zr}$ ($d_{5/2}$ ground-state) excitation function at 170° , centered on the $^{90}\text{Zr}(d,n)^{91}\text{Nb}$ ($d_{5/2}$ analog resonance) threshold. A large number of subsequent experiments have provided examples of similar anomalies in backward-angle ($>140^\circ$) (d,p) excitation functions, for targets $^{91,92,94,96}\text{Zr}$,²⁻⁴ $^{92,94}\text{Mo}$,³ ^{89}Y ,⁵ ^{88}Sr ,⁶ ^{80}Se ,⁷ and, also, perhaps ^{40}Ar ,⁸ ^{48}Ca ,⁹ and ^{52}Cr .¹⁰ In each case, an apparent dip in the cross section, about an MeV broad, is approximately centered on the appropriate (d,n) threshold. Various attempts to find similar effects using light-, other intermediate-, and heavier-weight nuclei have not been successful.¹¹

Faced with such a wealth of data, only partially suggested in Fig. 1, one must conclude that the reality of the threshold effect is demonstrated. However, the data have only begun to be analyzed theoretically,^{12,13} or even qualitatively interpreted. As a result, many aspects of the phenomenon remain unclear.

The simplest theoretical description of the threshold effect rests upon modification of the conventional distorted-wave Born-approximation (DWBA) amplitude by inclusion of the Lane potential¹⁴ in the optical potential of the exit channel. The usual exit channel, in which an outgoing proton with c.m. energy E_p leaves behind a neutron bound to the target, is thus coupled to the analogous channel, in which an outgoing neutron with

c.m. energy $E_n = E_p - \Delta_C$ leaves behind a proton in a resonant state which is the isobaric analog of the bound neutron state. Here, Δ_C is the Coulomb displacement energy of a single proton. The threshold deuteron energy at which the analogous (d,n) channel opens is, in the c.m. system, $E^{\text{th}}(d,p) = \Delta_C - Q(d,p)$, where $Q(d,p)$ is the (d,p) Q value for population of the appropriate residual state.

In this work, the reactions $^{90}\text{Zr}(d,p)$ and $^{91}\text{Zr}(d,p)$ have been extensively studied. The states of ^{91}Zr are basically single particle in character, while those of ^{92}Zr are collective. Since the threshold effect should not, in theory, depend on the nature of the residual state, other than indirectly through the proton decay properties of its isobaric analog,¹⁵ comparison of $^{90}\text{Zr}(d,p)$ and $^{91}\text{Zr}(d,p)$ results is instructive. The over-all aim is to investigate the scattering-angle dependence and the Q dependence (or residual-state dependence) of the threshold effect.

Unfortunately, there exist at present no (d,n) data for the analogs of the states excited in the (d,p) reactions. However, measurements have been made of the delayed protons from the decay of the analog state - i.e., the $(d,n\bar{p})$ reaction^{15,16} - and some information can thus be inferred concerning the total (d,n) cross section. Such information has been a useful guide both experimentally and theoretically¹³ in understanding the threshold effect in (d,p) .

Complementary data come from $(p,n\bar{p})$ measurements¹⁶ near the quasi-elastic (p,n) threshold. The $(p,n\bar{p})$ process has been extensively studied.¹⁷ Indeed, an apparent misconception of the nature of the (d,p) threshold anomaly led to several (unsuccessful) searches for "threshold effects" in proton

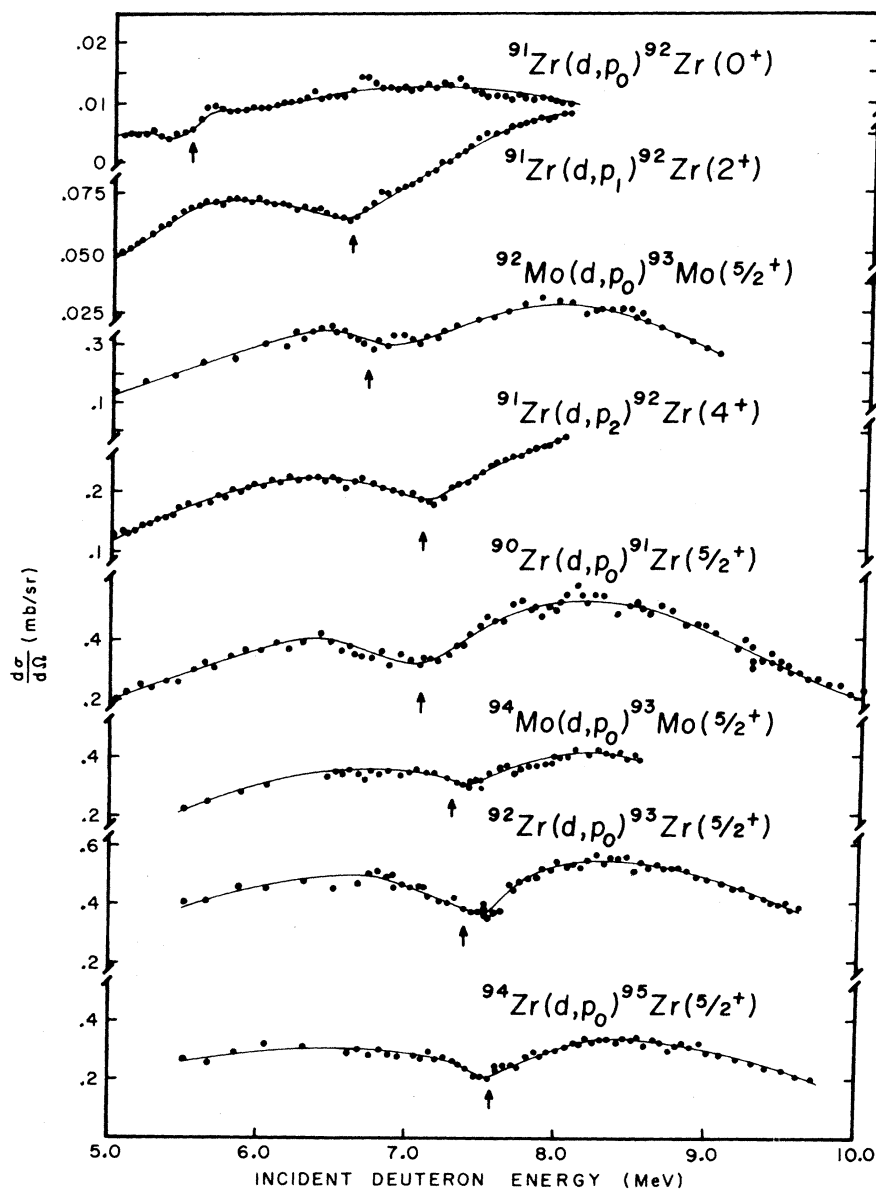


FIG. 1. A representative sampling of data on the (d, n) threshold effect in (d, p) excitation curves. Reading from top to bottom, the data shown are $^{91}\text{Zr}(d, p)$ (0^+ g.s. and 2^+ 0.93-MeV states) from Ref. 2 and the present work; $^{92}\text{Mo}(d, p)$ ($d_{5/2}$ g.s.) from Ref. 3; $^{91}\text{Zr}(d, p)$ (4^+ 1.49 MeV) from Ref. 2 and the present work; $^{90}\text{Zr}(d, p)$ ($d_{5/2}$ g.s.) from the present work; $^{94}\text{Mo}(d, p)$ ($d_{5/2}$ g.s.); $^{92}\text{Zr}(d, p)$ ($d_{5/2}$ g.s.) and $^{94}\text{Zr}(d, p)$ ($d_{5/2}$ g.s.) all from Ref. 3.

elastic scattering at the quasi-elastic (p, n) threshold. In the present work, we hope to clarify what is expected of $^{90}\text{Zr}(p, p)$ and $^{91}\text{Zr}(p, p)$ excitation functions near $E_p = \Delta_C$ in commenting upon our own data.

II. EXPERIMENTAL DETAILS

The targets were rolled metallic self-supporting foils, purchased from Oak Ridge National Laboratory, Separated Isotope Division. The ^{90}Zr and

^{91}Zr targets were enriched to 97.8 and 90.0%, respectively; target isotopic thicknesses were determined from low-energy, forward-angle, elastic proton and deuteron scattering. Measurements were made at several angles and energies to insure that the observed cross sections were due solely to Coulomb scattering. Various detectors were used to minimize systematic error from detector solid-angle measurements. Results obtained agree to within 7%. The target isotopic

thicknesses determined are: ^{90}Zr , 0.600 mg/cm², ^{91}Zr , 0.568 mg/cm².

The data to be discussed consist of excitation functions for the $^{90}\text{Zr}(d,p)$ reaction leading to the ground and eight excited states of ^{91}Zr , in the incident deuteron energy range from 5 to 11 MeV, at angles of 80, 95, 110, 140, 155, and 170°. Also, there are $^{90}\text{Zr}(p,p)$ excitation curves at 154, 164, 174° from 11.5 to 14.0 MeV, as well as $^{90}\text{Zr}(p,p)$ angular distributions at 10.75 and 12.7 MeV. Finally, there are deuteron elastic scattering angular distributions and excitation curves for selected energies and angles spanned by (d,p) measurements.

For the target ^{91}Zr , the data consist of $^{91}\text{Zr}(d,p)$ - $^{92}\text{Zr}(0^+$, ground state; 2^+ , 0.931 MeV; and 4^+ , 1.49 MeV) excitation curves at 160° from 4- to 8-MeV incident deuteron energy, previously published in preliminary form.² Also there is a $^{91}\text{Zr}(p,p)$ angular distribution at 10.75 MeV.

The $^{90}\text{Zr}(d,p)$ excitation-function data were accumulated with six 3-mm-thick Si(Li) detectors placed at lab angles of 80, 95, 110, 140, 155, and 170° with respect to the incident beam. The $^{91}\text{Zr}(d,p)$ excitation-function data were taken with two 3-mm-thick Si(Li) detectors placed at 160° on either side of the incident beam. The resulting

spectra were stored atop one another to double the count rate. Proton elastic angular distributions were taken at 10.75 MeV.

Details of the experimental arrangement are given in the following paper. Preliminary analysis of the spectra, as well as continuous data monitoring, were carried out automatically in an on-line PDP-7 computer by the program SUPERVISOR,¹⁸ which also wrote the data on standard IBM tapes. Final analysis was carried out from the tapes on the University of Texas CDC 6600 using the program DRAFT,¹⁹ which performed a least-squares fit of Gaussian peaks on a polynomial background to the desired region of the spectrum.

III. ELASTIC SCATTERING AND DWBA ANALYSES

An optical-model analysis was performed on the deuteron and proton elastic scattering data obtained in the experiment, as well as on the $^{90}\text{Zr}(p,p)$ angular distributions at 12.7 MeV taken by Dickens *et al.*²⁰ Final fits are shown in Fig. 2. A fairly unusual feature of the $^{90}\text{Zr}(d,d)$ analysis was the simultaneous fitting of the deuteron elastic excitation functions from 5.0 to 11.0 MeV, at 80, 95, 110, 140, 155, and 170°, as shown in Fig. 3, as well as the fitting of deuteron elastic angular dis-

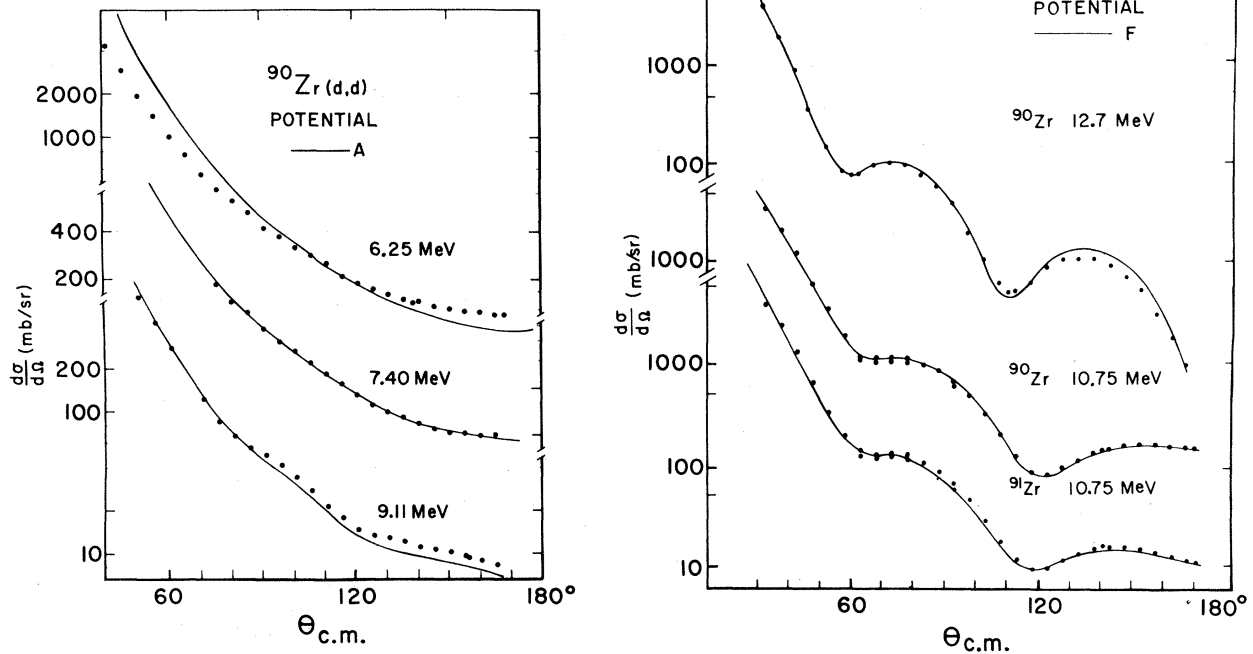


FIG. 2. Deuteron and proton elastic scattering angular distributions, with the fits given by potentials A and F of Tables I and II. The deuteron elastic scattering from ^{90}Zr was fit at 6.25, 7.4, and 9.11 MeV. The proton elastic scattering at 10.75 MeV from ^{90}Zr and ^{91}Zr , and at 12.7 MeV from ^{90}Zr (Ref. 19), are also shown, with fits.

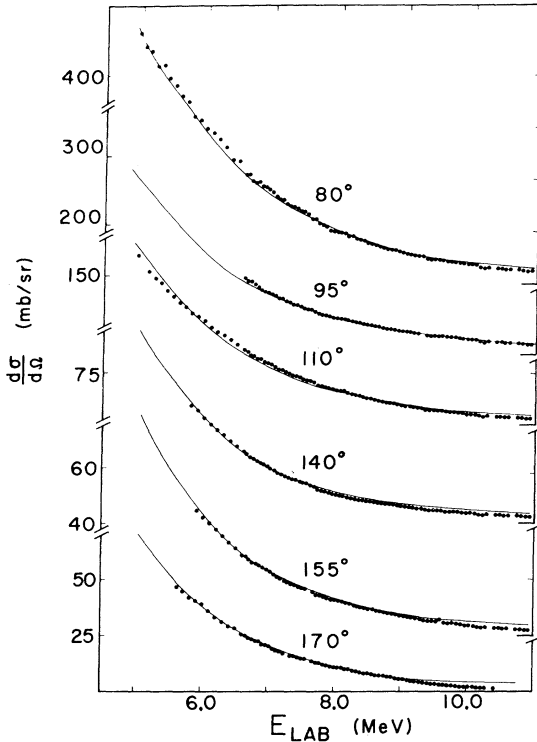


FIG. 3. Elastic scattering excitation functions for $^{90}\text{Zr}(d, d)$ at six angles, from 5 to 11 MeV, with a fit using potential A of Table I.

tributions taken at 6.25, 7.4, and 9.11 MeV to obtain a single, energy-dependent optical potential.

A literature search was also made, and the results are presented in Tables I and II. The reaction $^{90}\text{Zr}(d, p)^{91}\text{Zr}$ has been studied by a number of experimenters, at energies from 3.5 to 15 MeV. The tabulated optical potentials include those from our own analysis. It is amusing and instructive to

attempt to extract a single consistent potential from these tables.

For deuterons, one can use the " $V \times r_0^2 = \text{constant}$ " rule to adjust the tabulated real well depths crudely for a standard radius, here taken as 1.27 fm. The result is $V(E) = 91.1 \text{ MeV} - 0.44E_d$ with $r_0 = 1.27 \text{ fm}$ and $a_0 = 0.67 \text{ fm}$. The surface imaginary potential is seen to be generally constant at $W_D = 16.0 \text{ MeV}$, $r' = 1.39 \text{ fm}$, and $a' = 0.70 \text{ fm}$. A similar manipulation can be performed with the proton optical potentials of Table II, and one gets $V(E) = 58.4 \text{ MeV} - 0.42E_p$ with $r_0 = 1.23 \text{ fm}$ and $a = 0.63 \text{ fm}$, $W_D = 11.6 \text{ MeV}$, $r' = 1.25 \text{ fm}$, and $a' = 0.47 \text{ fm}$. For comparison, the average $^{90}\text{Zr}(p, p)$ potential from a recent survey by Greenlees²¹ using $r_0 = 1.17 \text{ fm}$ gives something like $V(E) = 54.5 - 0.32E_p$ when "converted" to $r_0 = 1.23 \text{ fm}$, $a_0 = 0.75 \text{ fm}$, thus differing by some 3 MeV in the region of interest. The deuteron and proton potentials actually used in our analysis are given as Sets A and F in Tables I and II.

The usual DWBA approach, using local potentials and the zero-range approximation (except for $l=0$ transitions), was taken in performing an analysis of the (d, p) excitation curves. As usual, the single-neutron bound states were Woods-Saxon states, bound at an energy equal in magnitude to the observed separation energy. For $s_{1/2}$ transitions, a finite-range approximation was made.²²

Nine states were observed in ^{91}Zr at excitation energies up to 3.70 MeV, and three states in ^{92}Zr at excitation energies up to 1.5 MeV. Excitation curves were obtained for all states, and DWBA calculations were performed for comparison with the data. From such a comparison, one hopes to learn:

- (1.) the true magnitude and extent of the anomalous behavior of the excitation functions near the

TABLE I. Optical-model parameters for elastic scattering of deuterons from $^{90, 91}\text{Zr}$.

| E (MeV) | V (MeV) | r_0 (fm) | a_0 (fm) | W_D (MeV) | r' (fm) | a' (fm) | V_{s_0} (MeV) | r'' (fm) | a'' (fm) | r_C (fm) | Ref. |
|--------------|--------------|---------------|---------------|----------------|--------------|--------------|--------------------|---------------|---------------|---------------|----------|
| 3.5 | 89.2 | 1.272 | 0.679 | 6.2 | 1.236 | 0.677 | 0 | ... | ... | 1.3 | a |
| 6.25 | 85.0 | 1.3 | 0.58 | 19.2 | 1.27 | 0.64 | 6.0 | 1.3 | 0.58 | 1.3 | 27 |
| | 88.0 | 1.28 | 0.72 | 15.95 | 1.39 | 0.70 | 0 | ... | ... | 1.3 | b, Set A |
| 7.4 | 85.6 | 1.28 | 0.72 | 15.95 | 1.39 | 0.70 | 0 | ... | ... | 1.3 | b, Set A |
| 9.11 | 83.5 | 1.28 | 0.72 | 15.95 | 1.39 | 0.70 | 0 | ... | ... | 1.3 | b, Set A |
| 10.0 | 87.84 | 1.27 | 0.56 | 8.81 | 1.53 | 0.985 | 0 | ... | ... | 1.3 | c |
| 10.8 | 88.56 | 1.2 | 0.88 | 14.65 | 1.35 | 0.723 | 0 | ... | ... | 1.2 | d |
| 11.0 | 94.5 | 1.235 | 0.65 | 23.10 | 1.046 | 0.65 | 3.86 | 1.235 | 0.65 | 1.235 | e |
| 11.8 | 85.4 | 1.272 | 0.679 | 18.39 | 1.236 | 0.677 | 0.0 | ... | ... | 1.272 | f |
| 15.0 | 90.0 | 1.23 | 0.64 | 12.0 | 1.18 | 0.93 | 0.0 | ... | ... | 1.30 | 23 |

^aC. E. Brient, E. L. Hudspeth, E. M. Bernstein, and W. R. Smith, Phys. Rev. **148**, 1221 (1966).

^bThis work.

^cJ. S. Forster *et al.*, Nucl. Phys. **101**, 113 (1967).

^dW. R. Smith, Phys. Rev. **137**, B913 (1965).

^eL. S. Michelman, S. Fiarman, E. J. Ludwig, and A. B. Robbins, Phys. Rev. **180**, 1114 (1969).

^fE. B. Dally, J. B. Nelson, and W. R. Smith, Phys. Rev. **152**, 1072 (1966).

TABLE II. Optical-model parameters for elastic scattering of protons from $^{90,91}\text{Zr}$.

| E (MeV) | V (MeV) | r_0 (fm) | a_0 (fm) | W_D (MeV) | r' (fm) | a' (fm) | V_{so} (MeV) | r'' (fm) | a'' (fm) | r_C (fm) | Ref. |
|--------------|--------------|---------------|---------------|-------------------|--------------|--------------|-------------------|---------------|---------------|---------------|----------|
| 8.5 | 53.0 | 1.25 | 0.65 | 12.0 | 1.25 | 0.47 | 0.0 | ... | ... | 1.25 | a |
| 10.75 | 53.5 | 1.22 | 0.607 | 5.76 | 1.29 | 0.74 | 7.5 | 1.22 | 0.607 | 1.25 | b, Set D |
| | 54.5 | 1.23 | 0.60 | 8.36 | 1.27 | 0.54 | 5.2 | 1.20 | 0.42 | 1.25 | b, Set E |
| | 55.0 | 1.25 | 0.65 | 14.5 | 1.25 | 0.47 | 6.8 | 1.20 | 0.42 | 1.25 | b, Set F |
| 12.7 | 52.8 | 1.25 | 0.65 | 15.6 | 1.25 | 0.412 | 6.0 | 1.25 | 0.65 | 1.25 | c |
| | 54.6 | 1.25 | 0.65 | 14.8 | 1.25 | 0.47 | 6.8 | 1.20 | 0.42 | 1.25 | b, Set F |
| | 54.2 | 1.22 | 0.607 | 5.4 | 1.29 | 0.737 | 7.9 | 1.22 | 0.607 | 1.25 | b, Set D |
| | 53.1 | 1.23 | 0.64 | 10.0 | 1.23 | 0.76 | 7.0 | 1.23 | 0.64 | 1.25 | 26 |
| 14.7 | 50.0 | 1.25 | 0.65 | 9.0 | 1.25 | 0.65 | 6.2 | 1.25 | 0.65 | 1.25 | d |
| | 52.7 | 1.224 | 0.65 | 9.35 | 1.254 | 0.65 | 5.5 | 1.224 | 0.65 | 1.224 | e |
| 15.0 | 52.4 | 1.23 | 0.623 | 4.54 ^f | 1.63 | 0.388 | 12.47 | 1.23 | 0.623 | 1.25 | g |
| | 51.7 | 1.23 | 0.633 | 8.03 | 1.31 | 0.649 | 12.17 | 1.23 | 0.633 | 1.25 | g |
| 16.0 | 54.3 | 1.20 | 0.716 | 11.7 | 1.26 | 0.548 | 0.0 | ... | ... | 1.25 | h |
| | 50.9 | 1.25 | 0.65 | 13.63 | 1.25 | 0.47 | 0.0 | ... | ... | 1.25 | i |
| | 55.6 | 1.19 | 0.65 | 7.73 | 1.31 | 0.65 | 7.0 | 1.19 | 0.65 | 1.19 | e |
| 18.7 | 51.5 | 1.24 | 0.65 | 12.27 | 1.28 | 0.50 | 6.78 | 1.20 | 0.42 | 1.25 | j |
| | 52.0 | 1.20 | 0.70 | 9.25 | 1.25 | 0.65 | 6.2 | 1.20 | 0.70 | 1.25 | k |
| 19.4 | 50.9 | 1.20 | 0.70 | 10.3 | 1.25 | 0.65 | 6.2 | 1.20 | 0.70 | 1.25 | l |
| 22.5 | 46.8 | 1.26 | 0.66 | 10.6 ^m | 1.23 | 0.567 | 7.75 | 1.26 | 0.664 | 1.25 | n |

^aC. E. Brient, E. L. Hudspeth, E. M. Bernstein, and W. R. Smith, Phys. Rev. 143, 1221 (1966).

^bThis work.

^cJ. K. Dickens, E. Eichler, and G. R. Satchler, Phys. Rev. 168, 1355 (1968).

^dK. Matsuda *et al.*, J. Phys. Soc. Japan 22, 1311 (1967).

^eL. S. Michelman, S. Fiarman, E. J. Ludwig, and A. B. Robbins, Phys. Rev. 180, 1114 (1969).

^fVolume-type (W).

^gJ. S. Forester *et al.*, Nucl. Phys. 101, 113 (1967).

^hW. R. Smith, Phys. Rev. 137, B913 (1965).

ⁱE. B. Dally, J. B. Nelson, and W. R. Smith, Phys. Rev. 152, 1072 (1966).

^jP. Kossanyi-Demay and R. de Swiniarski, Nucl. Phys. 108, 577 (1968).

^kW. S. Gray, R. A. Kenefick, and J. J. Kraushaar, Phys. Rev. 142, 735 (1966).

^lM. M. Stautberg and J. J. Kraushaar, Phys. Rev. 151, 969 (1966).

^mAlso, $W=0.5$ MeV; parameters from ^{92}Zr measurements.

ⁿJ. B. Ball, C. B. Fulmer, and R. H. Bassel, Phys. Rev. 135, B706 (1964).

- (d,n) threshold, in a given case;
 (2.) the dependence of the threshold effect on reaction angle;
 (3.) the dependence of the threshold effect on the excitation energy of the residual state (e.g., on the threshold energy itself).

IV. DISCUSSION OF RESULTS FOR ^{90}Zr TARGET

Excitation functions were obtained for the following states in ^{91}Zr : ground state $d_{5/2}$, 1.21 MeV $s_{1/2}$, 2.60 MeV $d_{3/2}$, 2.21 MeV $g_{7/2}$, 2.88 MeV $d_{3/2}$, 3.11 MeV $d_{3/2}$, 3.30 MeV $d_{3/2}$, 3.49 MeV $g_{7/2}$, and 3.70 MeV $d_{3/2}$. The configurations of the levels are quoted as assigned by Cohen and Chubinsky.²³ To summarize, a strong threshold anomaly, not explained by DWBA, is seen in the 155 and 170° excitation curves for the $d_{5/2}$ ground state. No such behavior is seen for the states of higher excitation, or other angles. Only the ground state, 1.21-, 2.06-, and 2.21-MeV states were completely analyzed with DWBA.

Figure 4 shows the $^{90}\text{Zr}(d,p)$ ($d_{5/2}$, ground-state) excitation curves. The 80, 95, and 110° curves show a simple structure, rising smoothly until $E_d \approx B_C$, the Coulomb-barrier height, then falling smoothly. The curves for 140, 155, and 170° show departures from this pattern, beginning at 7.05 MeV, the laboratory deuteron energy at which the (d,n) ($d_{5/2}$ analog) threshold opens. No attempts to account for this behavior by variation of the optical potentials of deuteron and proton in the DWBA amplitude were successful. It was not found possible to reproduce with DWBA the anomalous behavior of the ground-state excitation function, using proton and deuteron potentials which fit elastic scattering. Large arbitrary changes in the real or imaginary well depths of the optical potentials can certainly produce curious-looking excitation functions, but such calculations are physically meaningless. See the following paper for an example of the effect of the use of various realistic potential families on the calculated ground-state excitation function for $^{92}\text{Zr}(d,p)^{93}\text{Zr}$.

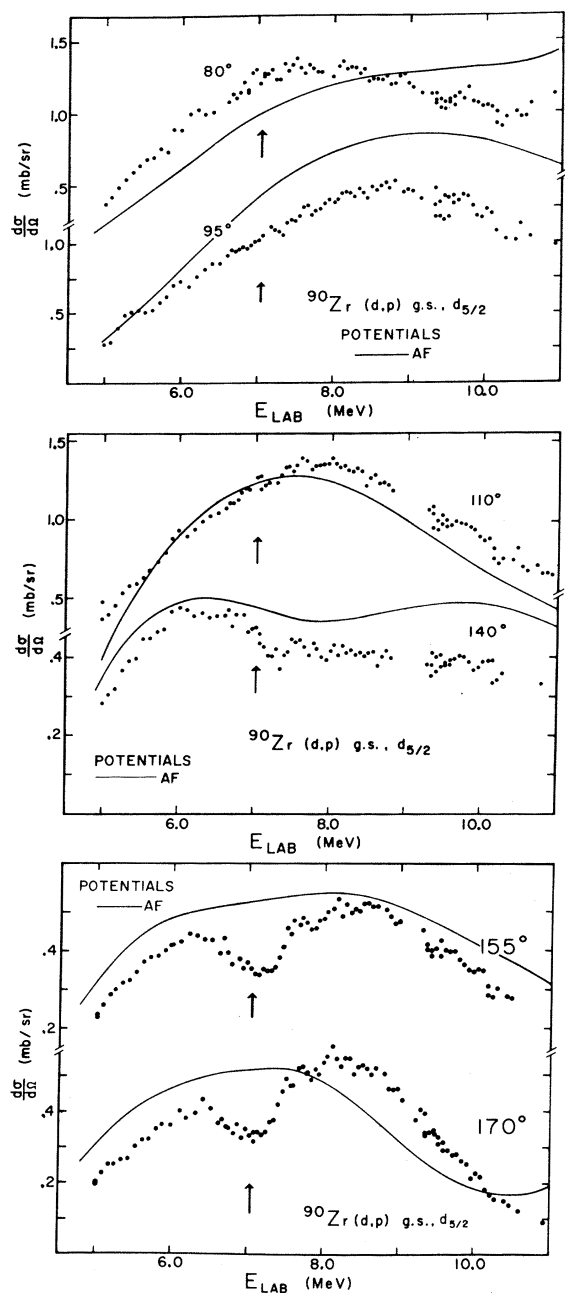


FIG. 4. Excitation functions of $^{90}\text{Zr}(d,p)$ ($d_{5/2}$ g.s.) at six angles, from 5 to 11 MeV, with a DWBA fit using potentials A and F from Tables I and II. Normalization is absolute.

In Fig. 5 are seen the $^{90}\text{Zr}(d,p)$ ($s_{1/2}$, 1.21-MeV) excitation curves. The familiar rising and falling behavior is again displayed by 80, 95, 110, and 140°. Only at 170° is there faint evidence of a departure from a smooth variation with energy, appearing near the (d,n) ($s_{1/2}$ analog) threshold at 8.25 MeV. The relative weakness or non-occur-

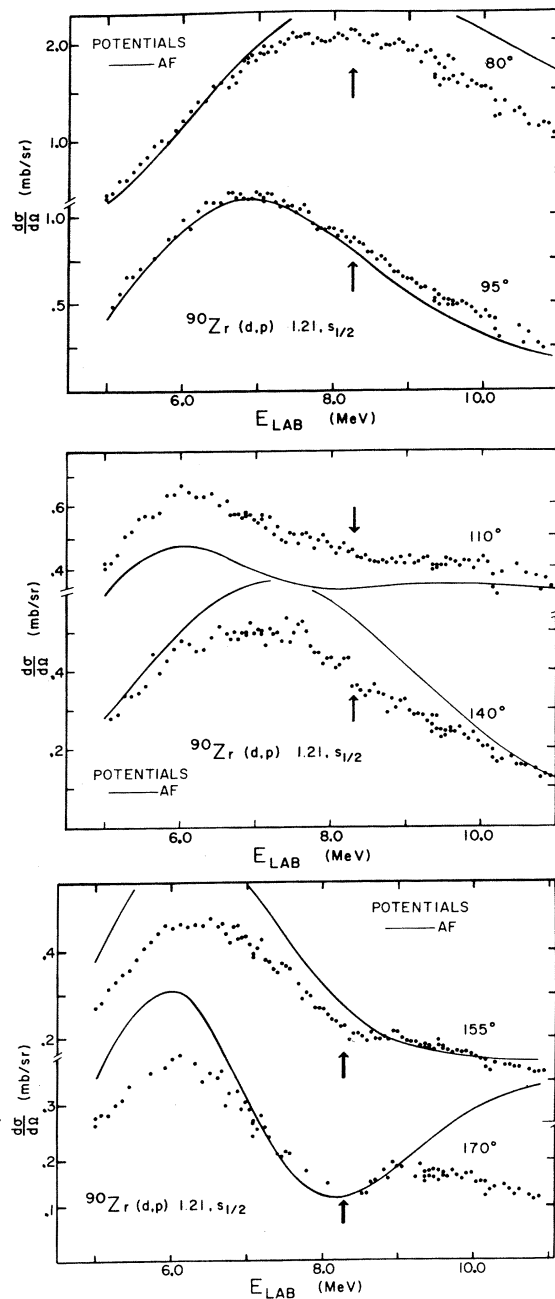


FIG. 5. Excitation functions of $^{90}\text{Zr}(d,p)$ ($s_{1/2}$, 1.21 MeV) at six angles, from 5 to 11 MeV, with a DWBA fit using potentials A and F from Tables I and II. Normalization is absolute.

rence of the effect, as compared with the $d_{5/2}$ case, is in accord with the $Q > \frac{1}{4}\Delta_C$ rule.¹³ The finite-range DWBA predictions are also shown in the figures, but fail to give a very satisfactory description of the data. They do show that the gross structure of the $s_{1/2}$ excitation curves can probably be described with DWBA.

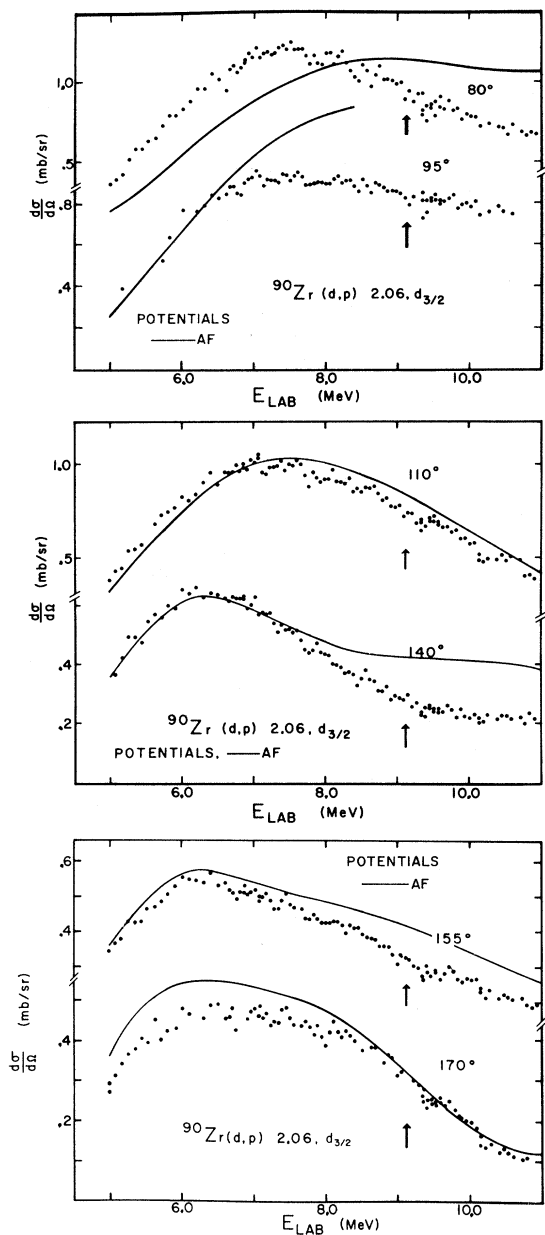


FIG. 6. Excitation functions of $^{90}\text{Zr}(d,p)$ ($d_{3/2}$, 2.06 MeV) at six angles, from 5 to 11 MeV, with a DWBA fit using potentials A and F from Tables I and II. Normalization is absolute.

In Fig. 6 are shown the excitation curves for the $^{90}\text{Zr}(d,p)$ ($d_{3/2}$, 2.06-MeV) reaction. Again the familiar behavior is in evidence at 80, 95, 110, 140, 155, and even 170°. Any effects due to charge exchange are so minor as to be invisible, and no unusual behavior is seen at the threshold, 9.1 MeV. Coupled-channel Born approximation (CCBA) calculations, which satisfactorily fit the $d_{5/2}$ and $s_{1/2}$ excitation curves, do not predict a noticeable anomaly in the $d_{3/2}$ state.¹³ Thus the data are so far in

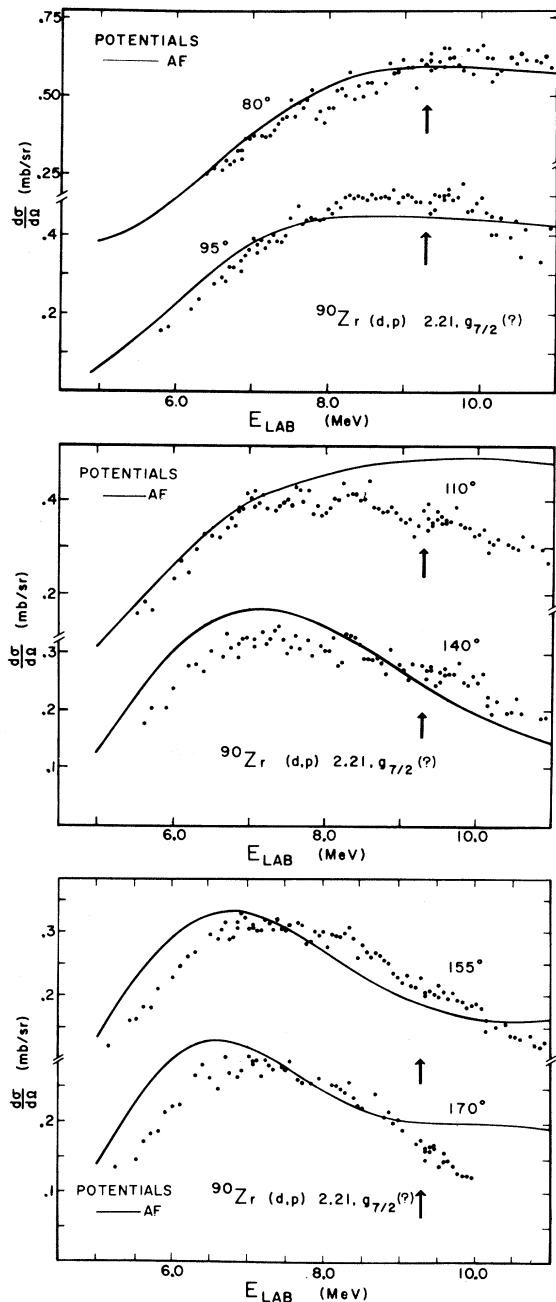


FIG. 7. Excitation functions of $^{90}\text{Zr}(d,p)$ ($g_{7/2}$, 2.21 MeV) at six angles, from 5 to 11 MeV, with a DWBA fit using potentials A and F from Tables I and II. Normalization is absolute.

excellent agreement with the theory. Note, indeed, that $Q(d_{3/2}) \approx 2.9$ MeV, while $\frac{1}{4}\Delta_C \approx 3.0$ MeV. The DWBA is seen to give a reasonable description of the data.

In Fig. 7 are shown the excitation curves for the $^{90}\text{Zr}(d,p)$ ($g_{7/2}$, 2.21-MeV) state. Again entirely "normal" behavior is expected and seen at all

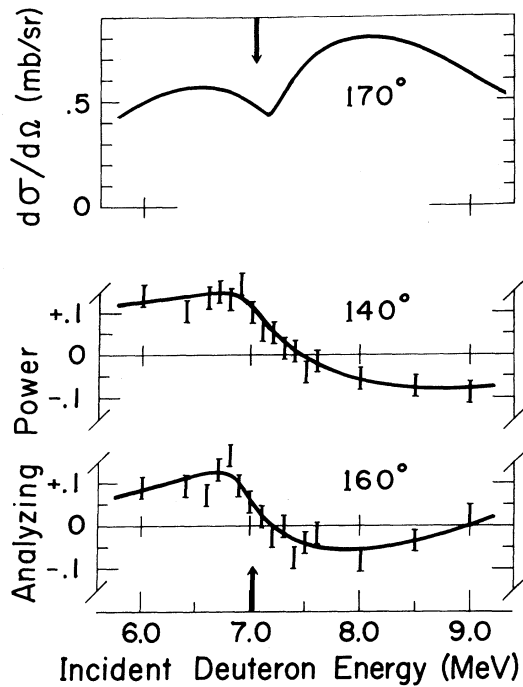


FIG. 8. Analyzing power of $^{90}\text{Zr}(d,p)^{91}\text{Zr}(d_{5/2}, \text{g.s.})$ at 140 and 160°, compared with the (d,p) cross section at 170° from Fig. 4. Analyzing power is here defined as $\frac{2}{3}$ the measured asymmetry divided by the deuteron polarization.

angles, and DWBA predictions are consistent with what is observed.

Because the anomalous behavior of the $d_{5/2}$ ground-state excitation function is so striking, it

is worthwhile to study in the threshold region either the polarization of the outgoing protons, or the asymmetry of the cross section using a polarized deuteron beam. Such an experiment has been performed using a vector-polarized deuteron beam. Experimental details are given by Clausnitzer *et al.*²⁴ The analyzing power was measured at 40, 60, 120, 140, and 160° from 6.0 to 9.0 MeV. As Fig. 8 indicates, the analyzing power as a function of energy displays an anomaly beginning near 7.05 MeV, at 140 and 160°. This result can be taken as an independent demonstration of the onset of a reaction mechanism other than direct (d,p) in the vicinity of the analogous (d,n) threshold. With the advent of more intense polarized beams, the analyzing power can be measured with greater accuracy. Studies of the inverse $^{91}\text{Zr}(p,d)$ reaction using polarized proton beams should also prove to be of interest. To date, DWBA calculations have not been able to provide a fit to the analyzing power at any angle.

Finally, proton elastic scattering excitation curves for ^{90}Zr are shown in Fig. 9, at 154, 164, and 174° from 11.5 to 14.0 MeV, spanning the quasi-elastic $^{90}\text{Zr}(p,n)^{90}\text{Nb}^A$ threshold at 12.0 MeV. No threshold effects are seen in these curves, a result again agreeing with predictions from coupled-channel calculations. Charge-exchange coupling of (p,p) and (p,n) channels cannot significantly affect many proton partial waves, and as a result the “resonating” (p,n) amplitude at threshold cannot make a significant contribution to the overwhelmingly larger (p,p) amplitude.

Such a situation is in sharp contrast to coupling

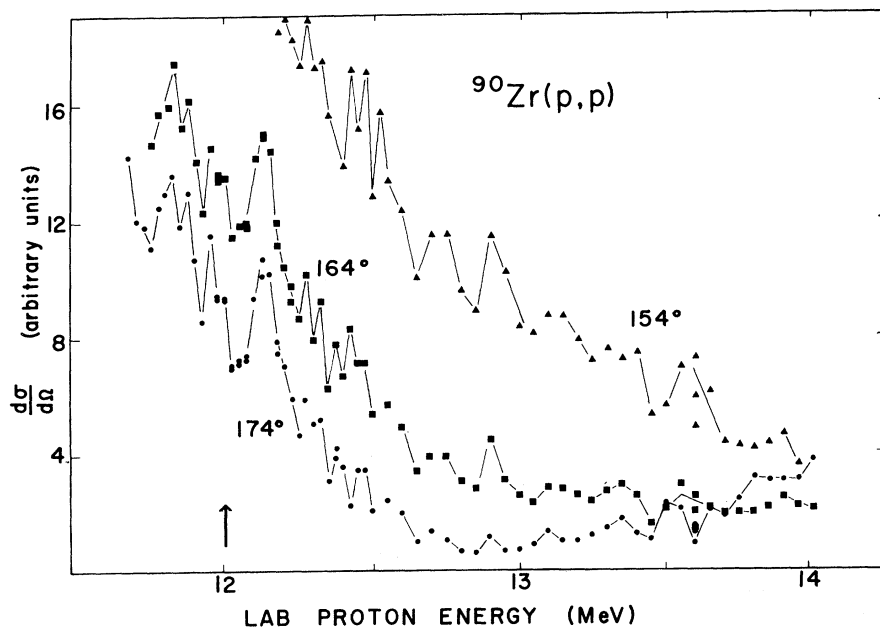


FIG. 9. Proton elastic scattering excitation functions at 154, 164, and 174°, from 11.5- to 14.0-MeV incident proton energy. The quasi-elastic $^{90}\text{Zr}(p,n)^{90}\text{Nb}^A$ threshold is indicated by the arrow.

for (d,p) , since, because of selection rules, relatively few deuteron and proton partial waves can contribute to the amplitude when the deuteron comes in below the Coulomb barrier, and a "resonating" (d,n) amplitude at threshold can affect the cross section noticeably at backward angles. This is the meaning of the $Q > \frac{1}{4}\Delta_C$ rule.¹³ When the (d,p) Q value is greater than $\frac{1}{4}\Delta_C$ then the threshold energy for the analogous (d,n) process is indeed less than the Coulomb-barrier height. Thus no observable effect of charge-exchange coupling in (d,p) is expected if $Q < \frac{1}{4}\Delta_C$.

It is interesting that what appear to be small p resonances have been seen at $E_p \approx \Delta_C$ in $^{96}\text{Zr}[(p,p), (p,p'), \text{ and } (p,d)]$ by Michelman, Bonner, and Kulleck⁴ and by Hinrichs *et al.*²⁵ in $^{98}\text{Mo}[(p,p), (p,d), \text{ and } (p,t)]$, as well as in $^{92}\text{Mo}(p,p)$ by Richard.²⁶ These resonances are presumably isobaric analogs of the just unbound, fractionated $p_{3/2}$ neutron state well known in the mass-90 region from thermal-neutron scattering. Figure 9 shows the $E_p = \Delta_C$ region of the 154, 164, and 174° excitation functions for $^{90}\text{Zr}(p,p)$. There is much small structure, but no dramatic dips as in ^{92}Mo and ^{96}Zr elastic excitation functions at $E_p = \Delta_C$.

In a similar connection, we should mention the (d,p) "fine structure" seen by Heffner *et al.*³ and studied in $^{90,92}\text{Zr}$ and ^{89}Y by Michelman and Moore.²⁶ A good example, from previously unpublished work,²⁷ is displayed in Fig. 10, showing the region including the $^{92}\text{Zr}(d,n)^{93}\text{Nb}(d_{5/2}, \text{g.s.})$ analog threshold in $^{92}\text{Zr}(d,p)^{93}\text{Zr}(d_{5/2}, \text{g.s.})$.³ Resonancelike behavior is seen near 7.36 MeV in both $^{92}\text{Zr}(d,p)^{93}\text{Zr}(d_{5/2}, \text{g.s.})$ and $^{92}\text{Zr}(d,p)^{93}\text{Zr}(s_{1/2}, 0.93\text{-MeV})$ excitation curves, and can therefore probably be attrib-

ted to compound-nuclear formation in the deuteron channel. Note that the "phase" is distinctively different for $d_{5/2}$ and $s_{1/2}$ "fine structure"; a dip in the former tends to line up with a rise in the latter. A remarkably similar phenomenon is observed in the $^{88}\text{Sr}(d,p)^{89}\text{Sr}(d_{5/2}, \text{g.s.})$ and $s_{1/2}, 1.05\text{-MeV}$ excitation functions of Zaidi, Coker, and Martin⁶; further investigation would seem warranted.

V. DISCUSSION OF RESULTS FOR ^{91}Zr TARGET

Excitation curves at 160° were obtained for $^{91}\text{Zr}(d,p)^{92}\text{Zr}$, leading to the 0^+ ground-state, 0.93-MeV 2^+ , and 1.49 MeV 4^+ states in ^{92}Zr , from 4.9 to 8.0 MeV. The data have been previously published,² as taken directly from the on-line PDP-7 analysis, and are reproduced in Fig. 11. Because of the high neutron binding energy, the Q values for population of all the three states are well above $\frac{1}{4}\Delta_C$, and a prominent threshold effect is expected in all the excitation functions: at 5.54 MeV for the 0^+ ground state, 6.48 MeV for the 0.93-MeV 2^+ state, and 7.04 MeV for the 1.49-MeV 4^+ state.

As Fig. 11 indicates, the expectation is well borne out. The appearance of the threshold effect in the 4^+ , 1.49 MeV state is strikingly similar to that in $^{90}\text{Zr}(d,p)(d_{5/2}, \text{g.s.})$, because of the similarity of the transitions (both $l=2$) and threshold energies. Because the 0^+ ground-state threshold occurs at so low an energy, and the corresponding analog resonance has a relatively small proton width, the result is simply the flattening of an already slowly rising curve, and is not too impressive without the DWBA as a reference. The DWBA calculations shown were done with the potentials

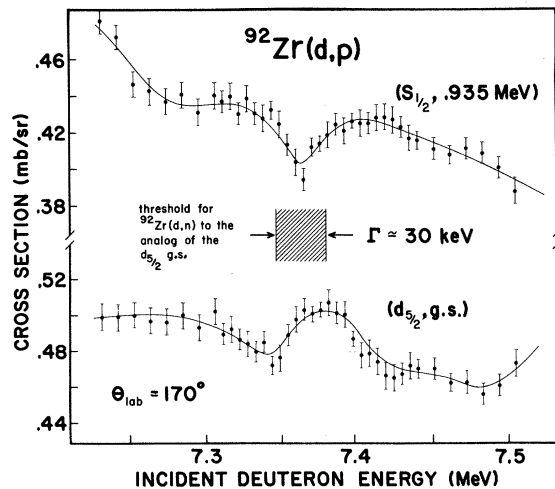


FIG. 10. An example of "fine structure" near the threshold for $^{92}\text{Zr}(d,n)^{93}\text{Nb}(d_{5/2}, \text{g.s.})$ analog, seen in both $^{92}\text{Zr}(d,p)(d_{5/2}, \text{g.s.})$ and $^{92}\text{Zr}(d,p)(s_{1/2}, 0.935\text{-MeV})$ excitation curves (see Ref. 29).

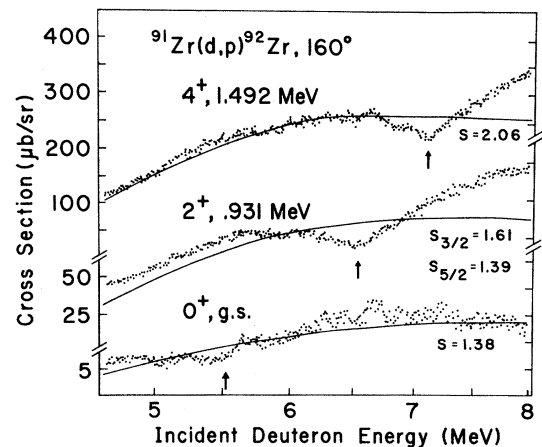


FIG. 11. Excitation curves for $^{91}\text{Zr}(d,p)^{92}\text{Zr}$, to the three lowest-lying states in ^{92}Zr , from 4.9- to 8.0-MeV incident deuteron energy. The solid curves are DWBA fits using the potentials of Tables I and II. Normalization is absolute. The quantities S are the normalizing factors used.

given by Dickens and Eicher.²⁸

Finally, excitation curves for proton elastic scattering on ^{91}Zr , from 10.2 to 13.0 MeV, at 154, 164, and 174° were obtained. Again, they show no threshold effects, but do show possible p -wave analog resonances at E_p (c.m.) $\approx \Delta_C$.

For completeness, we may summarize a study of the $^{91}\text{Zr}(p,d)^{90}\text{Zr}(0^+, \text{g.s.})$ and $^{91}\text{Zr}(p,n)^{91}\text{Nb}^A$ excitation functions at 165°, from 11 to 13 MeV, by Michelman and Moore.¹⁶ Time-reversal invariance requires the $^{91}\text{Zr}(p,d)^{90}\text{Zr}$ excitation curve to have exactly the same shape as the $^{90}\text{Zr}(d,p)^{91}\text{Zr}(d_{5/2}, \text{g.s.})$ excitation curve over an equivalent energy range, and also predicts the ratio of the two curves. Verification of these predictions is not very surprising. The remarkable difference between $(d,n\bar{p})$ and $(p,n\bar{p})$ excitation functions just above threshold is completely explained by consideration of the differing phase spaces of the two reactions. Indeed, the shape of the total cross section for either process, in the energy region from threshold to 1 or 2 MeV above, is readily fit assuming a constant transition amplitude.¹⁵ Figure 12 shows $^{90}\text{Zr}(d,n\bar{p})$ and $^{91}\text{Zr}(p,n\bar{p})$ data due to Michelman and Moore.¹⁶

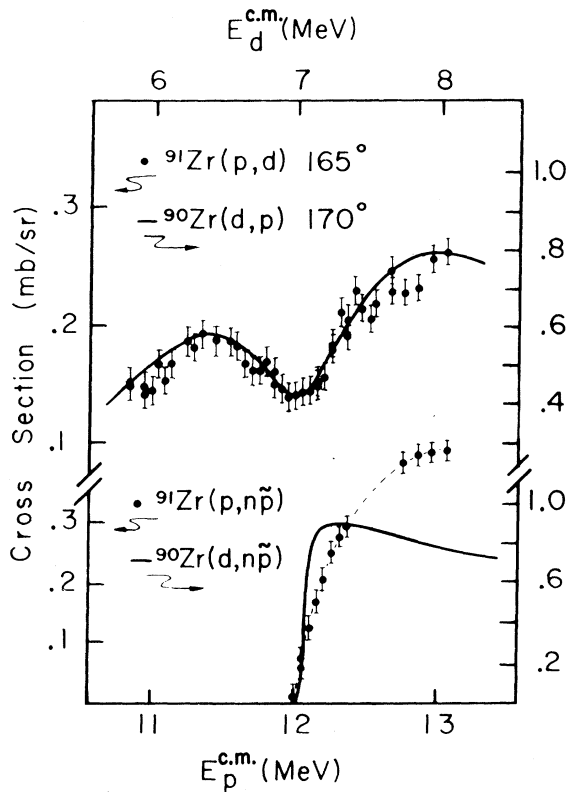


FIG. 12. A comparison of the present $^{90}\text{Zr}(d,p)$ - $(d_{5/2}, \text{g.s.})$ data with the $^{91}\text{Zr}(p,d)^{90}\text{Zr}(0^+, \text{g.s.})$ data of Ref. 15, and of the $^{90}\text{Zr}(d,n\bar{p})$ data of Ref. 1 and the $^{91}\text{Zr}(p,n\bar{p})$ data of Ref. 15 in the same energy region.

VI. OTHER TARGETS, $A \approx 50$

The s -wave neutron strength function peaks at about $A \approx 52$, which would therefore seem to be another possible mass region in which to investigate the threshold effect. Unfortunately, (d,p) excitation curves in the mass region of $A \approx 50$ show very large fluctuations at energies appropriate to threshold investigations. In order to remove the fluctuations, one is driven to averaging the data over intervals of 0.2 to 0.4 MeV. Such an average will also drastically weaken the threshold effect, if not remove it altogether, if it is the same size and shape near $A \approx 50$ as near $A \approx 90$.

Excitation-function data were taken at 160° for $^{56}\text{Fe}(d,p)^{57}\text{Fe}$ leading to states at 0.014, 0.136, 0.366, and 1.266 MeV in the energy region from 3.0 to 7.0 MeV. The analogs of all these states in ^{57}Cu are unbound. Because of the severe fluctuations in the cross section, however, the experiment

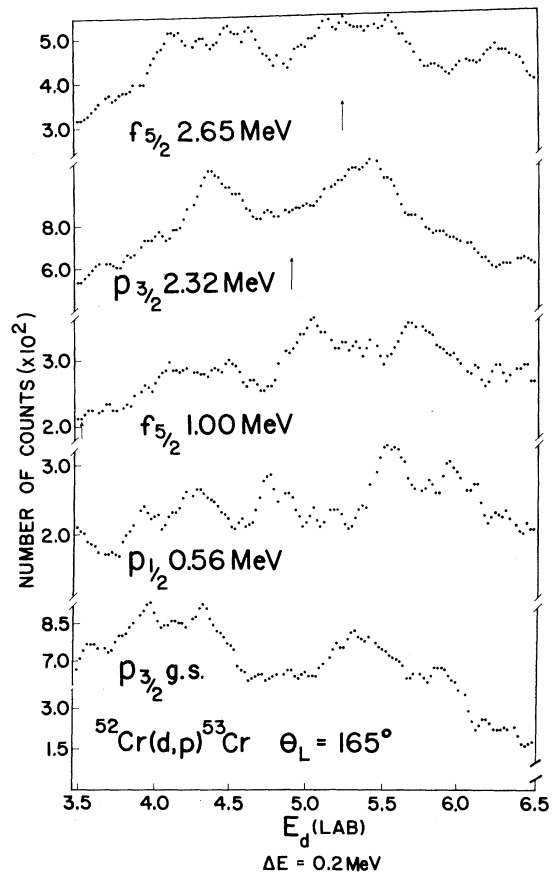


FIG. 13. Excitation functions for $^{52}\text{Cr}(d,p)^{53}\text{Cr}$ leading to five low-lying states in ^{53}Cr . The arrows indicate the position of the appropriate $^{52}\text{Cr}(d,n)^{53}\text{Mn}^A$ threshold. The data are averaged over an interval of 200 keV to remove fluctuations. The $p_{3/2}$ state at 2.32 MeV is the first to have an unbound analog in ^{53}Mn , and should be the first to show a threshold anomaly.

was inconclusive. Some evidence for threshold effects is found in the $^{40}\text{Ar}(d,p)^{41}\text{Ar}(d_{3/2}, 1.035\text{-MeV})$ excitation-function data of Cosack *et al.*,⁸ the $^{52}\text{Cr}(d,p)^{53}\text{Cr}(p_{3/2}, 2.32\text{-MeV})$ excitation-function data obtained by the present authors, and the $^{48}\text{Ca}(d,p)^{49}\text{Ca}(p_{3/2}, \text{g.s.})$ excitation-function data of Lacek, Bakowsky, and Strohmusch.⁹ The evidence is not, however, unambiguous, as previously unpublished $^{52}\text{Cr}(d,p)$ data, shown in Fig. 13, illustrate. The data shown are quite typical for $A \approx 50$.

VII. CONCLUSIONS

The experimental evidence presented in this and the following article is consistent with the conclusions of the early work,¹ and with the model suggested by Zaidi and von Brentano.¹⁴ In the mass-90 region, for (d,p) reactions populating states such that $Q(d,p) > \frac{1}{4}\Delta_C$, a dip is seen in the excitation function at the analogous (d,n) threshold. The size and width of the threshold dip depend upon several factors, apart from the obvious scattering-angle dependence:

- (1) the target mass, which determines (through the strength function) the amplitude of the resonating $l=1$ neutron partial wave, and therefore affects the size of the (d,n) amplitude contributing to (d,p) ;
- (2) the threshold energy, which determines how many deuteron partial waves can contribute significantly to the (d,p) and (d,n) amplitudes,^{12,13} and thus determines the relative importance of various outgoing neutron partial waves in their influence on the energy dependence of the (d,n) amplitude;
- (3) the decay properties of the residual analog

state, as measured for example by $(\Gamma/\Gamma_p^{1/2})$, where Γ is the total width and Γ_p the proton partial width. If Γ_p becomes too large, the three-body-breakup description of the $(d,n\bar{p})$ process becomes appropriate, and the direct sequential $(d,n)A^* \rightarrow p + C$ contribution to (d,p) becomes suppressed. This is almost certainly why no anomaly is seen for the $s_{1/2}$ transition in $^{90,92,94}\text{Zr}^{1,3}$ and $^{92,94}\text{Mo}$.³ No $s_{1/2} \bar{p}$ decay group was observed for $(d,n\bar{p})$ on these targets by Cue and Richard,¹⁵ suggesting that no strong sequential $(d,n)A^* \rightarrow \bar{p} + C$ process occurs for the $s_{1/2}$ analog states. It is clear that the nature of the analogous (d,n) process has an enormous effect on the appearance of the (d,p) anomaly, and no (d,p) -anomaly study is strictly complete without (d,n) cross sections.

It is difficult to disentangle the various influences on the threshold anomaly until a large amount of data on a wide variety of targets are carefully and systematically compared. In the data presented here, one mainly sees the influence of the second and third factors enumerated.

ACKNOWLEDGMENTS

The authors recognize the valuable assistance of J. J. Kent and J. G. Kulleck during the taking of data, and the labors of Jim Robertson in preparing many figures. Aid from Tom Henderson and Mary Jane Mikulas is also appreciated. One of us (RGC) gratefully acknowledges the support of a National Defense Education Act (Title IV) fellowship during the past three years.

*Research supported in part by the U. S. Atomic Energy Commission.

†Present address: Max-Planck-Institut für Kernphysik, Heidelberg, W. Germany.

¹C. F. Moore, C. E. Watson, S. A. A. Zaidi, J. J. Kent, and J. G. Kulleck, *Phys. Rev. Letters* **17**, 926 (1966).

²C. F. Moore, *Phys. Letters* **25**, 408 (1967).

³R. Heffner, C. Ling, N. Cue, and P. Richard, *Phys. Letters* **26**, 150 (1968); see also R. G. Clarkson and W. R. Coker, following paper, *Phys. Rev. C* **2**, 0000 (1970).

⁴L. S. Michelman, T. I. Bonner, and J. G. Kulleck, *Phys. Letters* **28**, 659 (1969).

⁵E. F. Alexander, C. E. Watson, and N. Shelton, to be published.

⁶S. A. A. Zaidi, W. R. Coker, and D. G. Martin, *Phys. Rev. C*, to be published.

⁷W. R. Coker and C. F. Moore, *Phys. Letters* **25**, 271 (1967).

⁸M. Cosack, M. K. Leung, M. T. McEllistrem, R. L. Schulte, J. C. Norman, M. M. Stautberg, and J. L. Weil, *Nucl. Phys.* **A136**, 532 (1969).

⁹H. Lacek, W. Bakowsky, and U. Strohmusch, *Z. Physik* **223**, 145 (1969).

¹⁰W. R. Coker and C. F. Moore, *Bull. Am. Phys. Soc.* **13**, 631 (1968).

¹¹L. L. Lee, Jr., J. W. Olness, and R. H. Siemssen, *Bull. Am. Phys. Soc.* **12**, 1197 (1967); P. Wilhelm, G. A. Keyworth, G. C. Kyker, D. L. Sellin, N. R. Roberson, and E. G. Bilpuch, *Phys. Rev. Letters* **18**, 130 (1967); R. G. Clarkson and C. F. Moore, work on $^{56}\text{Fe}(d,p)$ (unpublished); C. F. Moore, F. Boreli, R. G. Clarkson, B. B. Kinsey, and S. A. A. Zaidi, *Bull. Am. Phys. Soc.* **12**, 33 (1967); P. von Brentano, J. G. Cramer, R. Heffner, R. Hinrichs, and P. Richard, 1968 Annual Report, Nuclear Physics Laboratory, University of Washington (unpublished), p. 43.

¹²T. Tamura and C. E. Watson, *Phys. Letters* **25**, 183 (1967).

¹³W. R. Coker and T. Tamura, *Phys. Rev.* **182**, 1277 (1969).

¹⁴A. M. Lane, *Nucl. Phys.* **35**, 676 (1962); see also S. A. A. Zaidi and P. von Brentano, *Phys. Letters* **23**, 446 (1966); J. Zimanyi and B. Gyarmati, *ibid.* **27**, 120 (1968); and M. B. Hooper, in *Proceedings of the Second*

Conference on Nuclear Isospin, Asilomar-Pacific Grove, 1969, edited by J. D. Anderson, S. D. Bloom, J. Cerny, and W. True (Academic Press Inc., New York, 1969).

¹⁵N. Cue and P. Richard, *Phys. Rev.* **173**, 1108 (1968).

¹⁶L. S. Michelman and C. F. Moore, *Phys. Letters* **26**, 446 (1968).

¹⁷A. I. Yavin, R. A. Hoffswell, L. H. Jones, and T. M. Noweir, *Phys. Rev. Letters* **16**, 1049 (1966).

¹⁸R. G. Clarkson, Technical Report No. 3, Center for Nuclear Studies, University of Texas (unpublished).

¹⁹R. G. Clarkson and C. E. Watson, unpublished.

²⁰J. K. Dickens, E. Eicher, R. J. Silva, and G. Chilosi, Oak Ridge National Laboratory Report No. ORNL-3934 (unpublished).

²¹F. D. Becchetti, Jr., and G. W. Greenlees, *Phys. Rev.*

182, 1190 (1969).

²²P. J. A. Buttle and L. J. B. Goldfarb, *Proc. Phys. Soc. (London)* **83**, 701 (1964).

²³B. L. Cohen and O. V. Chubinsky, *Phys. Rev.* **131**, 2184 (1963).

²⁴G. Clausnitzer, G. Graw, C. F. Moore, and K. Wienhard, *Phys. Rev. Letters* **22**, 793 (1969).

²⁵R. A. Hinrichs, G. W. Phillips, J. G. Cramer, and H. Wieman, *Bull. Am. Phys. Soc.* **14**, 121 (1969).

²⁶P. Richard, private communication.

²⁷L. S. Michelman and C. F. Moore, unpublished.

²⁸J. K. Dickens and E. Eicher, *Nucl. Phys.* **101**, 408 (1967).

²⁹R. G. Clarkson and W. R. Coker, following paper [*Phys. Rev. C* **2**, 1108 (1970)].

Charge Exchange in $^{92}\text{Zr}(d,p)^{93}\text{Zr}^\dagger$

R. G. Clarkson* and W. R. Coker

Center for Nuclear Studies, The University of Texas, Austin, Texas 78712

(Received 30 July 1969; revised manuscript received 11 June 1970)

Excitation functions for the $^{92}\text{Zr}(d,p)^{93}\text{Zr}$ reaction to eight low-lying states in ^{93}Zr were measured from 4.2- to 11.2-MeV incident deuteron energy, a region including the (d,n) thresholds to the analogs of the observed states. Charge-exchange effects were observed for at least the $d_{5/2}$ ground state in ^{93}Zr . Also, $^{92}\text{Zr}(d,d)$ angular distributions were taken at 6.25, 7.5, and 11.0 MeV, in 5° steps from 40 to 165° , in order to obtain deuteron optical parameters. A $^{92}\text{Zr}(p,p)$ angular distribution was taken at 10.75-MeV proton energy in order to obtain proton optical parameters. Orbital angular momenta and estimates of spectroscopic factors were obtained for three previously unreported states in ^{93}Zr . The results of distorted-wave Born-approximation calculations for the excitation curves are discussed.

1. INTRODUCTION

A cusplike behavior exhibited in (d,p) excitation functions for several nuclei, almost all in the mass-90 region, has been the subject of several recent experimental investigations.¹⁻⁶ Such behavior is always observed near the threshold for the (d,n) reaction to the isobaric analog of the final state observed in the (d,p) reaction, and has been attributed to charge-exchange coupling.⁷⁻⁹ In particular, $^{90}\text{Zr}(d,p)$ has been extensively studied^{1,2}; also, to a lesser extent, (d,p) reactions on ^{91}Zr , ^{92}Zr , and ^{94}Zr have been studied.^{1,2,4-6} Results of some of these investigations are discussed in Ref. 1.

In this article, we report on a study of $^{92}\text{Zr}(d,p)^{93}\text{Zr}$, including optical-model analysis of elastic scattering at appropriate energies in deuteron and proton channels, excitation functions for all observed states, and a complete distorted-wave Born-approximation (DWBA) analysis. Figure 1 shows a level diagram of the observed states in ^{93}Zr and their analogs in ^{93}Nb . The present work is a continuation and extension of the earlier investigations,

with the aim of making a thorough experimental study of the charge-exchange effect for a particular case and providing information regarding the isotopic systematics of the effect.

2. EXPERIMENTAL METHOD

The deuteron and proton beams for this experiment were obtained from the 12-MeV model-EN tandem Van de Graaff accelerator at the Center for Nuclear Studies, University of Texas at Austin. A beam of approximately $0.3 \mu\text{A}$ on target was used during most of the experiment. The beam energy spread was estimated to be less than 4 keV. Deuteron beams of energies from 4 to 11 MeV, and a proton beam of 10.75 MeV, were used. The beam energy was controlled by a 90° analyzing magnet, with the usual nuclear-magnetic-resonance probe. The magnet was calibrated using the $^{27}\text{Al}(p,n)$ threshold at 5.803 MeV.

The ^{92}Zr target was a rolled self-supporting foil, purchased from Oak Ridge National Laboratory, Separated Isotope Division, and enriched to 94.6% ^{92}Zr . The target isotopic thickness was determined